AD-A130 107 HF SATELLITE ANTENNA ANALYSIS(U) ROME AIR DEVELOPMENT 1/1
CENTER GRIFFISS AFB NY B WEIJERS OCT 82 RADC-TR-82-230

UNCLASSIFIED F/G 9/5 NL

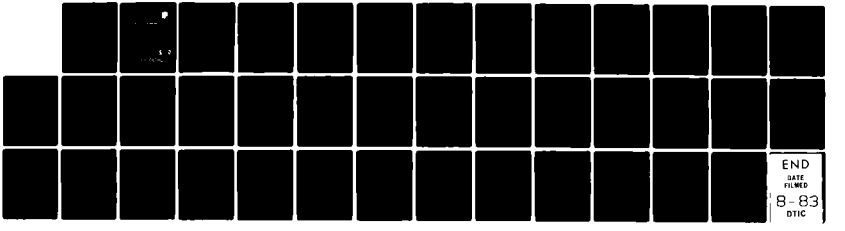

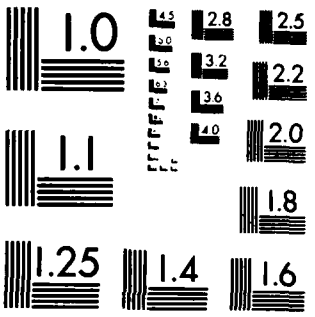

RADC-TR-82-230
In-House Report
October 1982

HF SATELLITE ANTENNA ANALYSIS

Bertus Weijers

ROME AIR DEVELOPMENT CENTER
Air Force Systems Command
Griffiss Air Force Base, NY 13441

This report has been reviewed by the RADC Public Affairs Office (PA) and is releasable to the National Technical Information Service (NTIS). At NTIS it will be releasable to the general public, including foreign nations.

RADC-TR-82-230 has been reviewed and is approved for publication.

APPROVED: Terence J. Elkins

TERENCE J. ELKINS
Chief, Propagation Branch

APPROVED: Allan C. Schell

ALLAN C. SCHELL
Chief, Electromagnetic Sciences Division

FOR THE COMMANDER: John P. Huss

JOHN P. HUSS
Acting Chief, Plans Office

If your address has changed or if you wish to be removed from the RADC mailing list, or if the addressee is no longer employed by your organization, please notify RADC (EEPI) Hanscom AFB MA 01731. This will assist us in maintaining a current mailing list.

Do not return copies of this report unless contractual obligations or notices on a specific document requires that it be returned.

Unclassified

SECURITY CLASSIFICATION OF THIS PAGE (When Data Entered)

REPORT DOCUMENTATION PAGE		READ INSTRUCTIONS BEFORE COMPLETING FORM
1. REPORT NUMBER RADC-TR-82-230	2. GOVT ACCESSION NO. AD-A130107	3. RECIPIENT'S CATALOG NUMBER
4. TITLE (and Subtitle) HF SATELLITE ANTENNA ANALYSIS		5. TYPE OF REPORT & PERIOD COVERED In-house
		6. PERFORMING ORG. REPORT NUMBER
7. AUTHOR(s) Bertus Weijers		8. CONTRACT OR GRANT NUMBER(s) N/A
9. PERFORMING ORGANIZATION NAME AND ADDRESS Rome Air Development Center (EEPI) Hanscom AFB MA 01731		10. PROGRAM ELEMENT, PROJECT, TASK AREA & WORK UNIT NUMBERS 62702F 46001608
11. CONTROLLING OFFICE NAME AND ADDRESS Rome Air Development Center (EEPI) Hanscom AFB MA 01731		12. REPORT DATE October 1982 13. NUMBER OF PAGES 39
14. MONITORING AGENCY NAME & ADDRESS(if different from Controlling Office)		15. SECURITY CLASS. (of this report) Unclassified 15a. DECLASSIFICATION DOWNGRADING SCHEDULE N/A

16. DISTRIBUTION STATEMENT (of this Report)

Approved for public release; distribution unlimited.

17. DISTRIBUTION STATEMENT (of the abstract entered in Block 20, if different from Report)

18. SUPPLEMENTARY NOTES

19. KEY WORDS (Continue on reverse side if necessary and identify by block number)

High frequency
Ionosphere
Satellite antenna

20. ABSTRACT (Continue on reverse side if necessary and identify by block number)

Results of a satellite antenna analysis using the Antenna Modelling Program (AMP) are presented. A satellite structure with an HF dipole antenna attached was simulated using a wire grid model. The HF dipole antenna is part of a receiving system in earth orbit used for an ionospheric ducted mode experiment. The antenna gain patterns for several possible satellite antenna configurations are presented and analyzed to determine acceptable configurations for the ducted mode experiment. Examined were the influence of dipole element length, orientation of the elements, and their positioning with respect

DD FORM 1 JAN 73 1473 EDITION OF 1 NOV 65 IS OBSOLETE

Unclassified

SECURITY CLASSIFICATION OF THIS PAGE (When Data Entered)

20. Abstract (contd)

to the satellite structure for frequencies from 6 to 30 MHz. Also, the antenna impedances were calculated to determine the possible losses when the antenna is terminated in a resistive impedance load. The influence of the ionospheric plasma on the mismatch losses was also estimated.

Preface

I wish to thank Dr. Gary S. Sales for his reading and suggestions for the improvement of this paper, and special thanks to SSgt Jacqueline J. Wilson for her help in the implementation of the Antenna Modelling Programs.

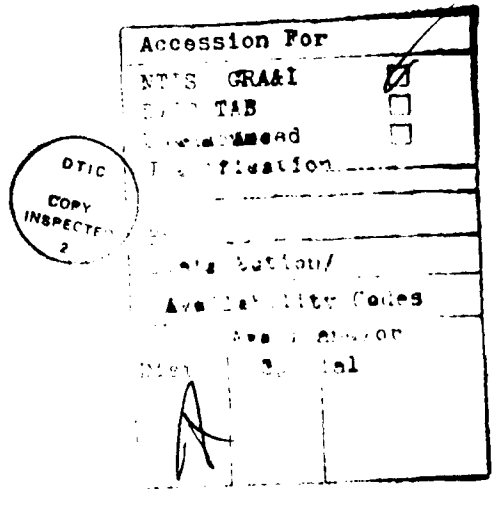

Contents

Illustrations

Illustrations

HF Satellite Antenna Analysis

1. INTRODUCTION

An experimental program is planned to verify the possibility of using non-classical ionospheric propagation modes (ducted and chordal) for long-range surveillance and communications systems. For this purpose, a receiving system will be placed in an Earth orbiting satellite (Figure 1) to make direct measurements of duct parameters at altitudes were ducting is most likely to occur in the ionosphere. HF radio signals (6 to 30 MHz) from a ground transmitter will be scattered from field-aligned irregularities into the ducts for reception by the satellite receiver. The parameters considered in the antenna-satellite relationship were location of the antenna and length and orientation of the antenna elements.

Antenna gain patterns and characteristic impedances were calculated using the Antenna Modelling Program (AMP).[1] This experiment requires a satellite antenna configuration that has a relatively constant response over the frequency range to be investigated (6 to 30 MHz). The pattern should have a null in the downward direction, necessary to avoid overloading of the receiver when directly passing over powerful ground-based transmitters, and uniformity of the horizontal

(Received for publication 8 December 1982)

1. (1974) Antenna Modelling Program, Engineering Manual, MBA, San Roman, California.

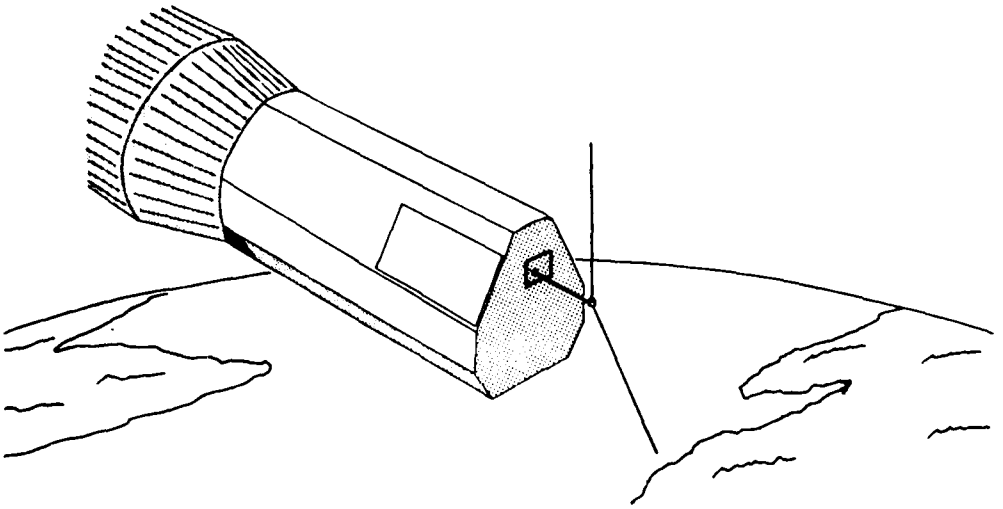

Figure 1. Possible Configuration of Satellite and Antenna

gain pattern to insure reception of ducted signals from all azimuthal directions. Also determined was the influence of impedance matching of antenna to receiver on the received signal-to-noise ratio (SNR).

2. ANTENNA MODELLING PROGRAM

The antenna gain patterns and corresponding impedances were calculated using the AMP.[1] This program was developed for antenna analysis as a joint effort of Navy, Army, and Air Force (RADC). AMP uses the thin wire electric field integral equation, which relates the exciting field to the induced currents on a specified wire geometry. The integral equation is reduced to a system of simultaneous linear algebraic equations in terms of the unknown current. Each wire is divided into N segments with the current being an unknown constant over each segment. The integral equation is solved numerically by writing N equations in N unknowns.

The unknown current vector is related to the excitation vector by a coefficient matrix that depends only on the geometry of the structure where the matrix equations are solved for by using the Gauss-Doolittle elimination procedure. Field patterns are calculated by summing the contributions of the N currents.

Virtually all calculations involved in analyzing the electrical response of a structure to an excitation takes place in the subroutines of AMP (Figure 2). The

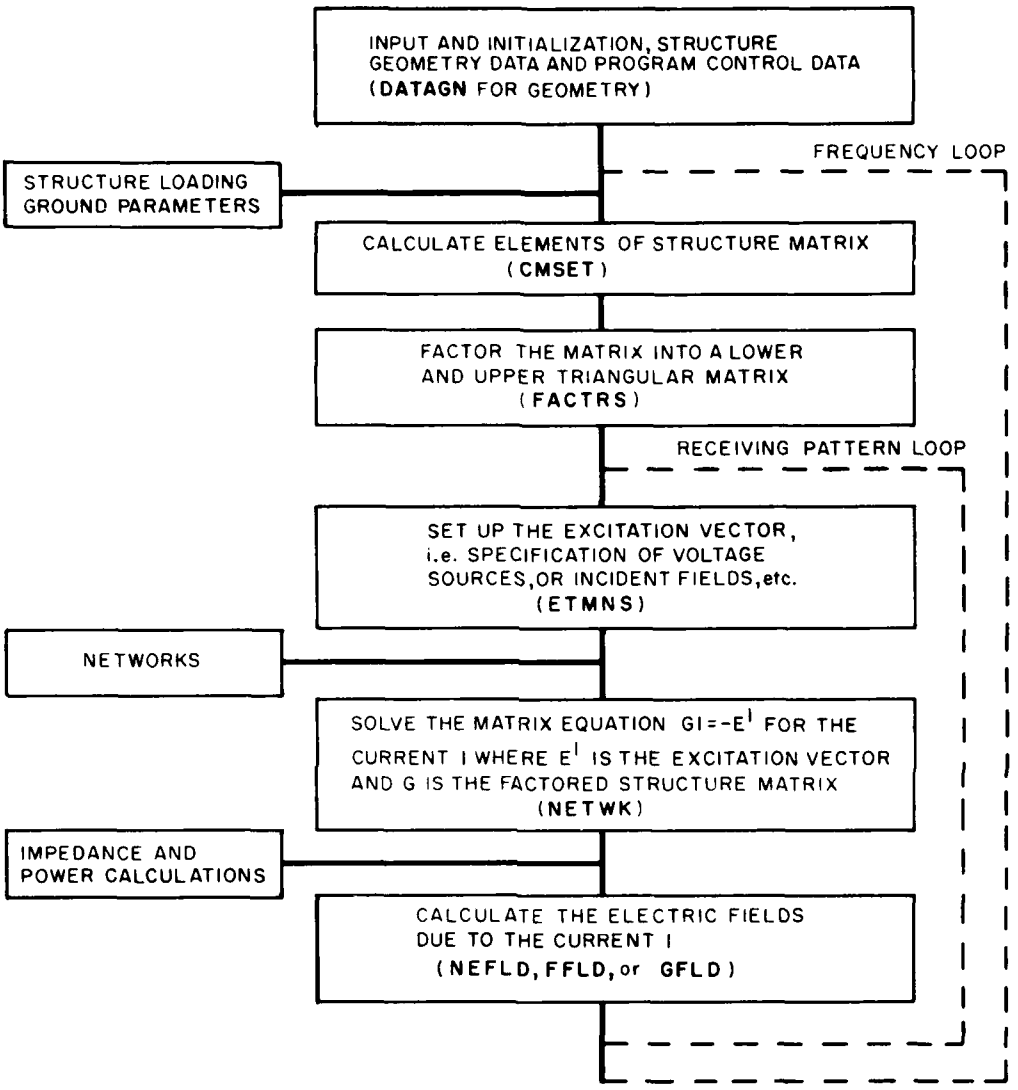

Figure 2. Block Diagram of AMP Program

primary functions of the main program are to control the logical flow between one subroutine and the next and to handle the data input and output for the user. The output of the program is a gain function:

$$G_d(\theta, \phi) = \frac{4\pi P_\Omega(\theta, \phi)}{P_{in}} ,$$

where

$P_\Omega(\theta, \phi)$ = power radiated per unit solid angle

P_{in} = total power accepted by the antenna .

The radiation pattern of the antenna in the program is specified in terms of the far electric field, $E(\theta, \phi)$. As a function of the polar coordinate angles θ and ϕ, the radiation intensity is proportional to the square of the E field and the directivity D. Thus

$$D = \frac{E_{max}^2}{\frac{1}{4\pi} \iint E^2(\theta, \phi)\, d\Omega} ,$$

where $d\Omega$ is a differential element of solid angle. In polar coordinates this expression becomes

$$D = \frac{4\pi E_{max}^2}{\int_0^{2\pi} \int_0^{\pi} E^2(\theta, \phi) \sin\theta d\theta d\phi} .$$

This equation defines the directivity with respect to a lossless isotropic radiator. Power gain G is related to this expression by the relation

$$G = k \cdot D ,$$

where k = the efficiency of the antenna. The efficiency of an antenna is less than unity due to heat loss caused by the finite conductivity of the elements and the losses of the associated dielectric structure.

An equivalent loss resistance (R_{loss}) will appear such that the terminal resistance of an antenna is given by $R = R_{loss} + R_r$. Then

$$k = \frac{\text{Power Radiated}}{\text{Power Input}} = \frac{R_r}{R_r + R_{loss}}$$

where R_r = radiation resistance. For many types of antenna systems the loss resistance is very low and the value of the power gain is essentially the same as the directive gain. The efficiency of the satellite antenna in these calculations is assumed to be unity.

3. SATELLITE MODELLING AND INPUT PARAMETERS

The satellite antenna and body were modelled using a wire grid model (Figure 3). Each wire used in the model is subdivided into segments. The modelling accuracy depends on the number and the density of these wire segments. Results become more accurate when the size of the segments is decreased. But the number of segments directly influences the computing time. The time needed to fill the current matrix is proportional to the square of the number of segments, and the matrix solving time is proportional to the cube of the number of segments.[1]

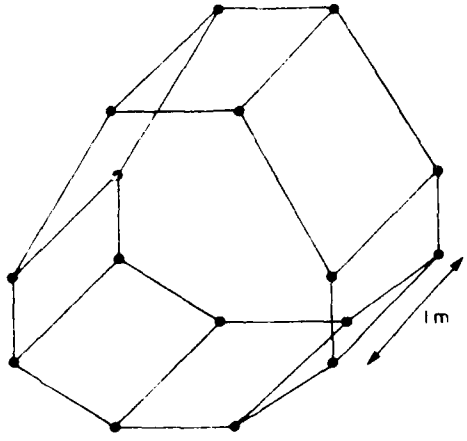

Figure 3. Section of Wire Grid Model Satellite Body

Segment lengths may vary over the structure but have to be selected according to certain rules. Sudden changes in length of adjacent elements should be avoided. This is especially important at junctions of several wires where segment length ratios should be kept within a factor of about 2. Also the radius of the wire should always be less than 0.1 x segment length. In these calculations a radius of 0.00625 m was used. Generally the segment length should be less than 0.1 x wavelength at the desired frequency. Shorter segments were used in modelling critical regions, such as the "bend" between the antenna elements in Figure 6. The basic wire grid model shown in Figure 3, was used to generate all other sections of the satellite model until the desired overall length was obtained (Figures 4 and 5).

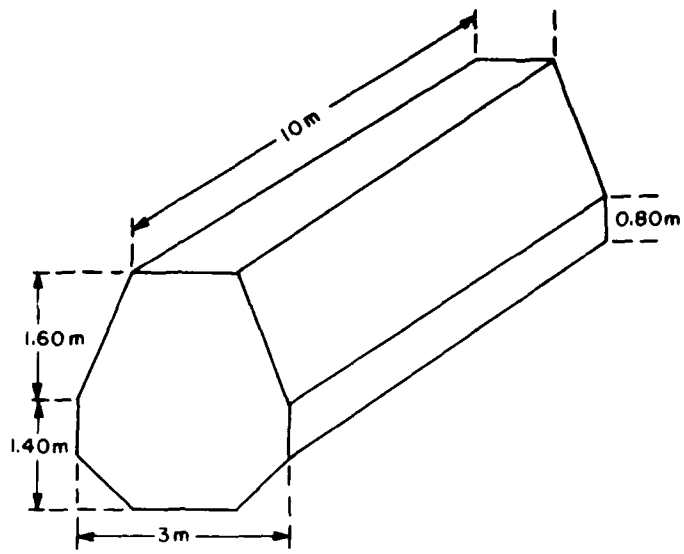

Figure 4. *Dimensions of Satellite Model*

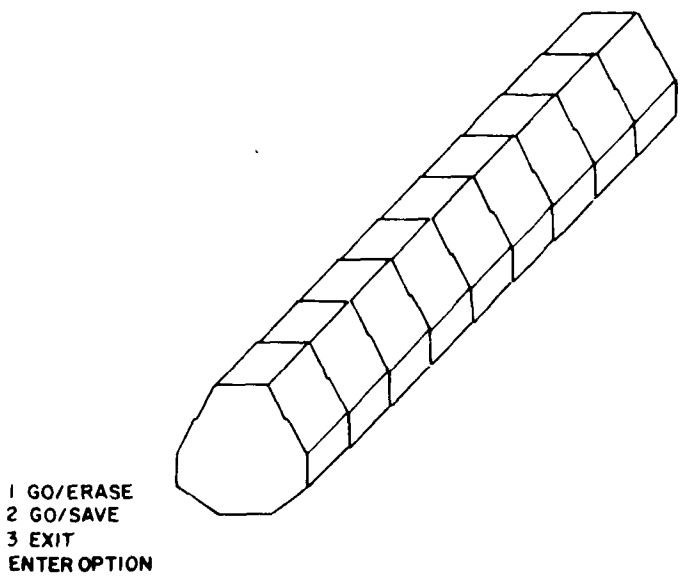

Figure 5. Computer-Generated Extended Satellite Structure

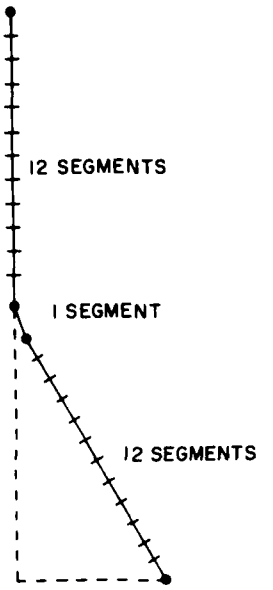

Figure 6. Segmentation of Satellite Antenna Elements

When using AMP to determine gain, impedance, etc., antenna models can only be analyzed for the transmitting cases. *AMP can still be used because the* results for gain and impedance are the same for receiving and transmitting antennas by reciprocity. If the wire model is used as a receiving structure the AMP output will give the scattered power per unit area. The gain patterns were determined relative to an isotropic radiator for the horizontal plane and the vertical plane. These two planes are sufficient for this analysis, because the orientation of the patterns on a stabilized satellite will not change with respect to the earth. Frequencies used for the calculations were 6, 10, 15, 20, 25, and 30 MHz.

4. SATELLITE ANTENNA CONFIGURATIONS

The satellite configurations considered in this analysis are shown in Figure 7 and described here. The dimensions given in Figures 4 and 7 are those used in AMP calculations. The different configurations will only be identified by the letter used in Figure 7 when referred to in the following descriptions.

Configuration a has elements of each 3 m long, with the upper element parallel to the vertical axis, and the lower element inclined from the vertical by

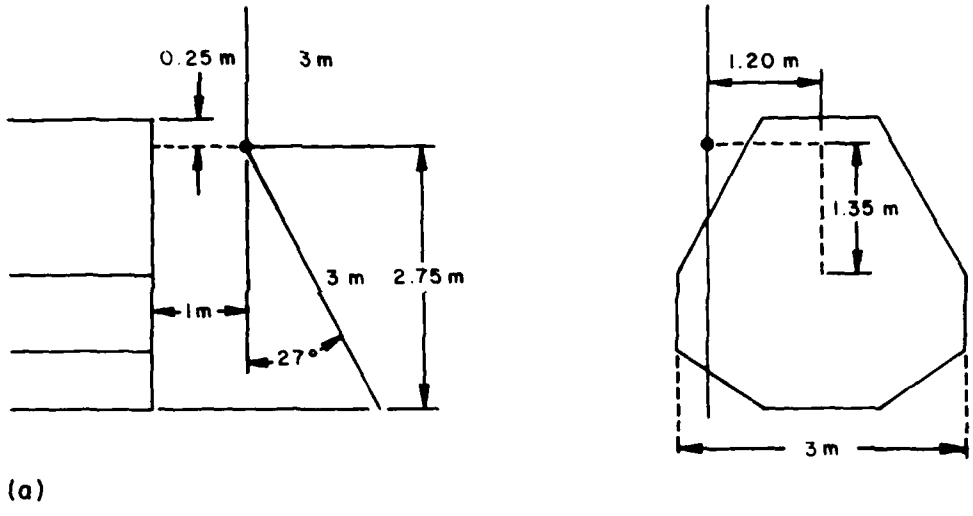

(a)

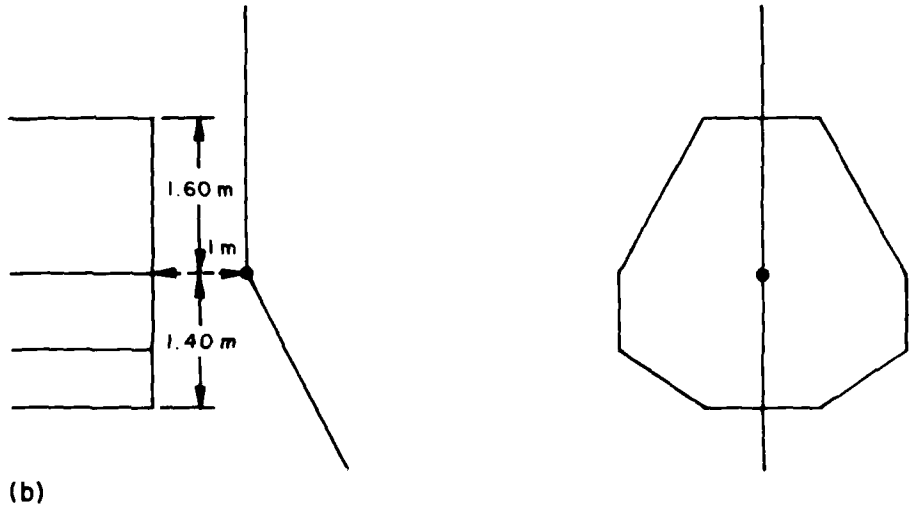

(b)

Figure 7. Satellite Antenna Configurations. (a) Off-center, (b) center, (c) asymmetric elements, (d) symmetric elements, length 2.5 m, (e) symmetric elements, length 3.0 m, and (f) symmetric elements, length 1.5 m, off-center

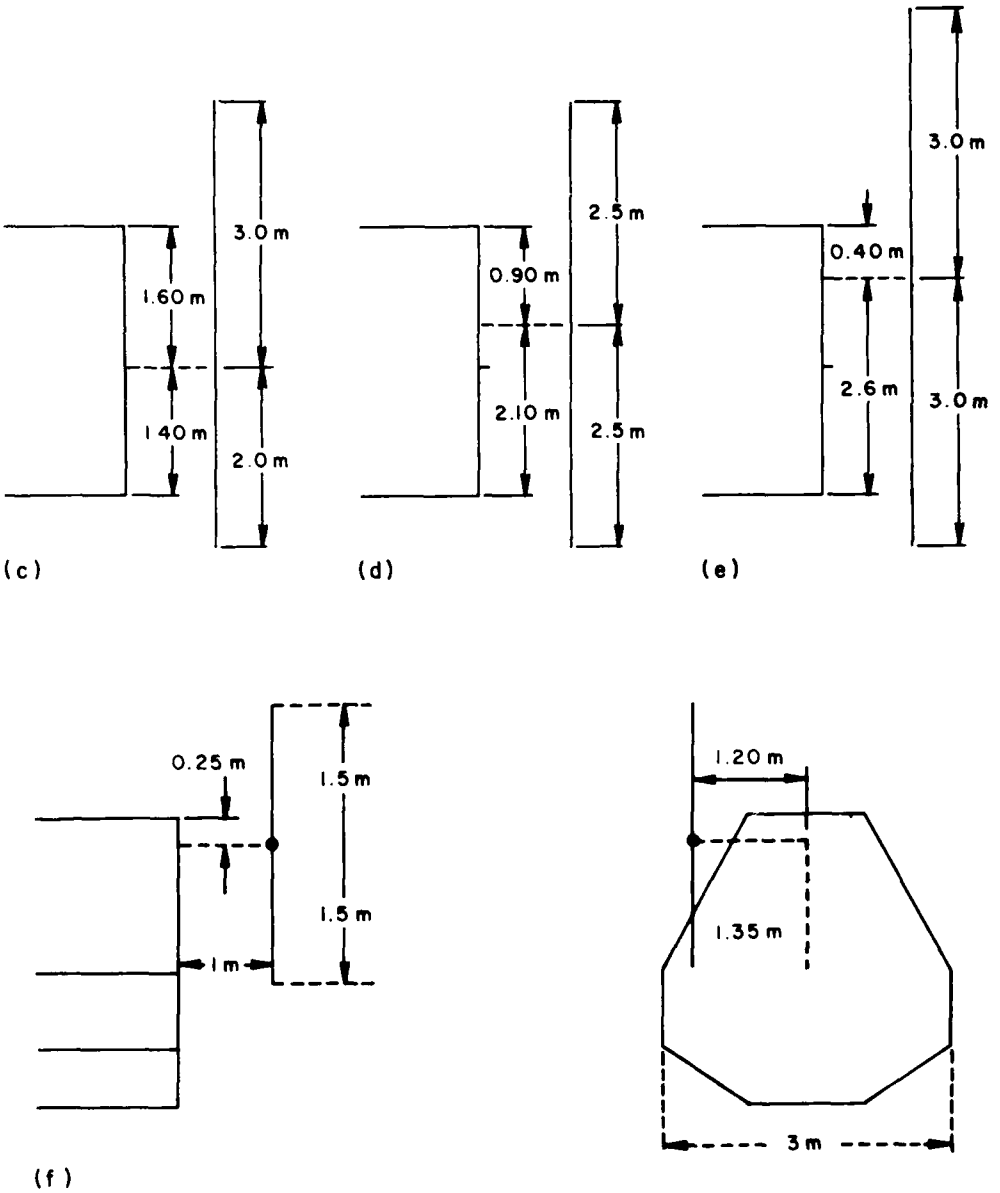

Figure 7. Satellite Antenna Configurations. (a) Off-center, (b) center, (c) asymmetric elements, (d) symmetric elements, length 2.5 m, (e) symmetric elements, length 3.0 m, and (f) symmetric elements, length 1.5 m, off-center (Contd)

27^{o}. The vertical axis of the antenna and the front bulkhead of the satellite are separated by 1 m.

In configuration b the vertical axis of the antenna coincides with vertical center line of the satellite structure. Configuration b has elements similar in size and positioning to configuration a.

Both configurations a and b are based on figures obtained from the preliminary Interface Control Document. As shown in Figure 8, both antennas have the lower element inclined from the vertical axis to avoid interference with the field of view in the downward direction of the host vehicle. The configuration in Figure 8(b) appeared as the one having the greatest impact on this field-of-view (FOV) and was therefore used as the basis for an assumed restricted zone into which elements of the antenna cannot extend.

The antenna in Figure 8(b) is placed away from the vertical center line of the satellite structure, and as exact dimensions and final placement were not known, configuration b was considered a reasonable model for analysis. Also from configuration b the restricted zone was determined by connecting the lowest point on the front of the bulkhead to the extreme tip of the lower antenna element. This restricted zone (Figure 9) was taken into consideration in the following configurations:

Antenna configurations c, d, and e were analyzed to determine the effect of the inclined element on the orientation of the null with respect to the vertical axis, having both upper and lower elements parallel to the vertical axis. The presence of the restricted zone required that the element size had to be changed and, when necessary, the antenna moved upward on the vertical center line. Configuration c is therefore asymmetric with a lower element of 2 m and an upper element of 3 m. The antenna terminals are located as in configuration b. Configurations d and e are symmetric with element lengths of each 2.5 m and 3 m respectively. Both antennas have their centers moved upward to avoid the restricted zone.

Configuration f is a symmetric dipole with elements only 1.5 m long and parallel to the vertical axis. The center of the dipole is in the same location as in configuration a. This configuration was used to determine the effect of the satellite structure on the antenna gain pattern and impedance of an antenna with shortened elements.

5. RESULTS OF ANTENNA GAIN PATTERN CALCULATIONS

The directive gain patterns of the antenna configurations (Figure 10) examined appeared similar to the patterns of a simple dipole antenna when the dimensions

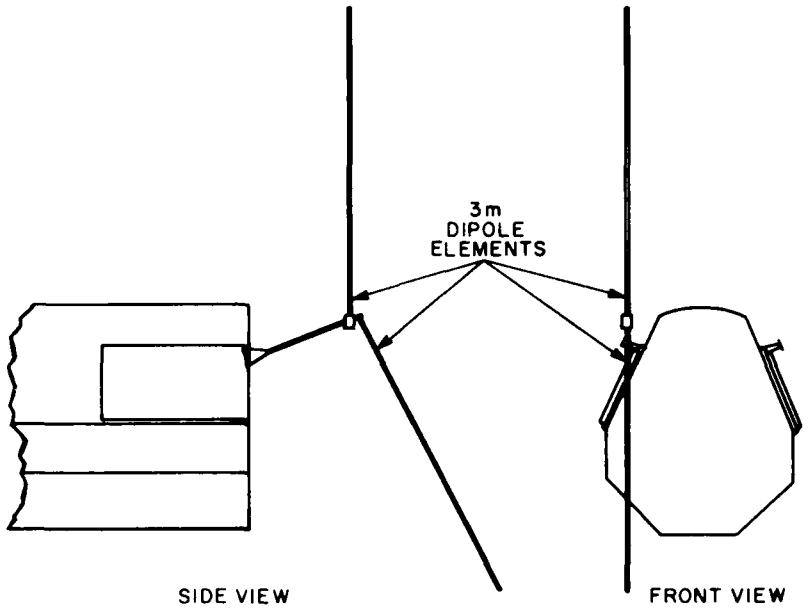

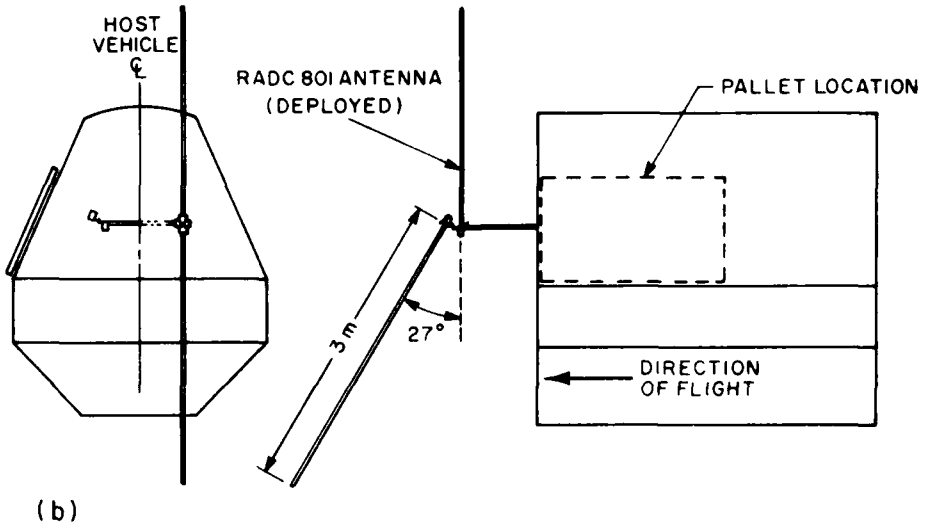

Figure 8. Satellite Configurations from Contractor I. C. D. (a) Off-center and (b) center

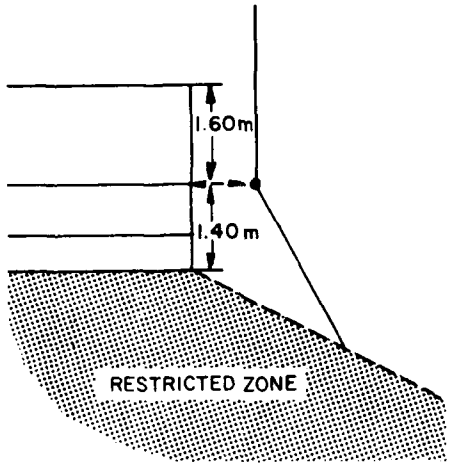

Figure 9. Assumed Restricted Zone Using Dimensions From Configuration b (Figure 7)

were small in terms of wavelength. The null in the vertical plane pattern was tilted with respect to the vertical axis due to the reflecting surface presented by the front bulkhead of the satellite. Antenna patterns for configurations a and b are presented in Figure 11(a)-11(f) as a function of frequency. The null in the downward direction for configuration a is at least 9 dB below the horizontal gain except at the two lower frequencies of 6 and 10 MHz. The gain pattern in the horizontal (azimuthal) plane has an ideal circular shape for both configurations a and b. At the highest frequency used, 30 MHz, the horizontal plane plot has a less circular shape.

Configuration c, using the asymmetric element, has an attenuation of at least 12 dB down from the horizontal plane Figure 12(a)-12(c) except for the 10 MHz configurations. The horizontal plane plots for these configurations are similar to those of configurations a and b. Configurations d and e, both symmetric antennas, show vertical gain plots with the nulls remaining tilted with respect to the vertical axis. At 15 MHz the gain in the downward direction for both configurations d and e is 10 dB and 7 dB down from the horizontal gain (Figure 13). Downward-looking attenuation improved with increasing frequency and the attenuation for both the d and e configurations was better than 25 dB down at 30 MHz.

Configuration f, with 1.5 m symmetrical elements, had a pattern shown in Figure 14(a)-14(c) that was greatly influenced by the presence of the satellite structure. The vertical plane plot had only a 5 dB vertical attenuation null at 15 MHz. The other frequencies show equally undesirable patterns resulting from this configuration.

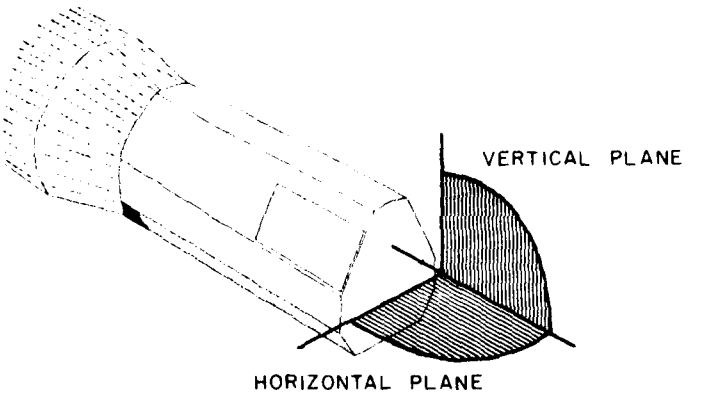

Figure 10(a)

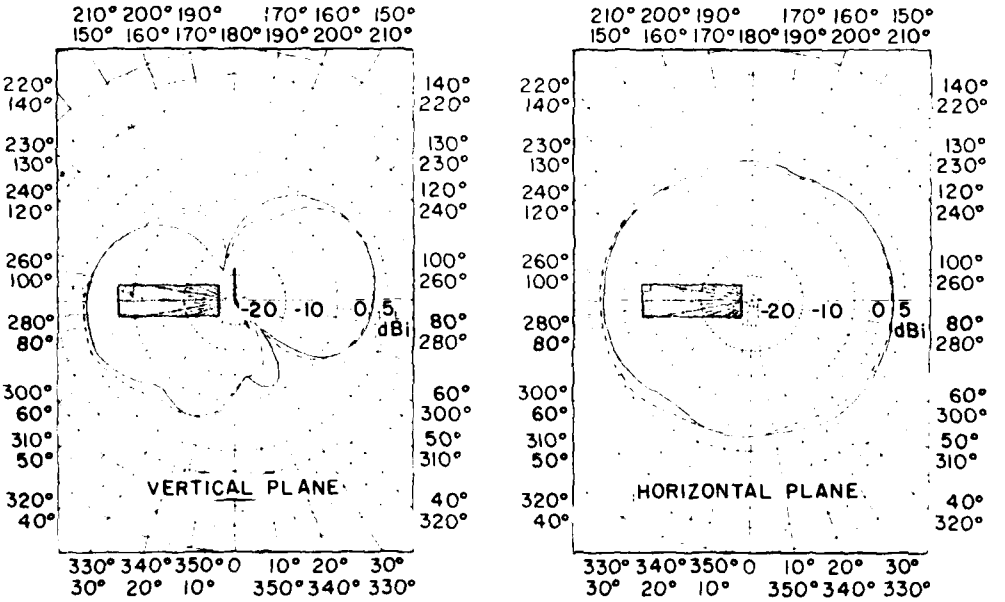

Figure 10(b)

Figure 10. Planes of Analysis of Antenna Gain Pattern. (a) Horizontal and vertical plane with respect to satellite structure and (b) orientation of the satellite structure in horizontal and vertical plane plots

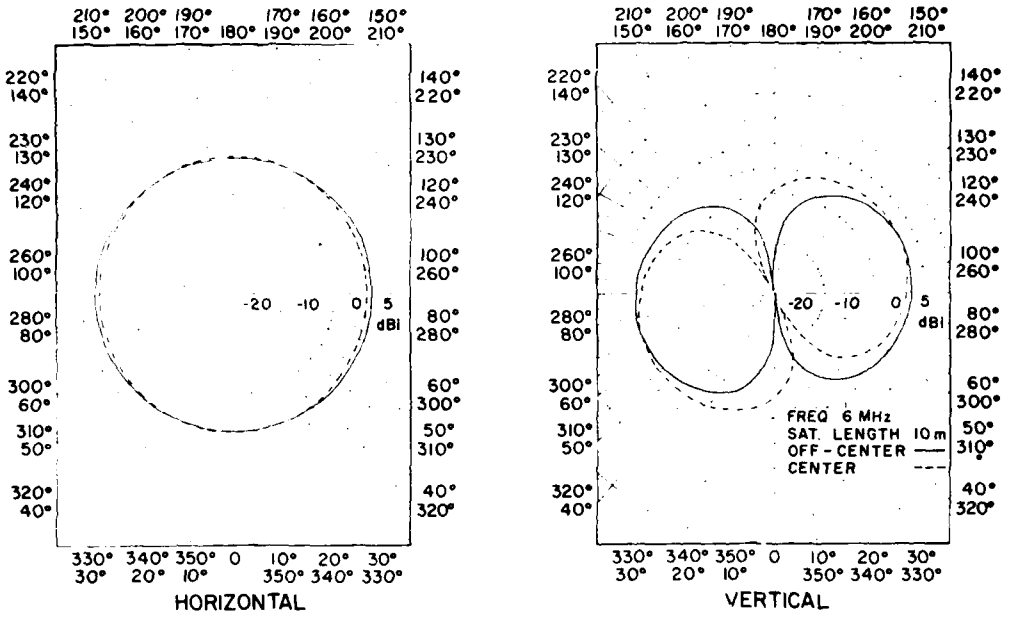

Figure 11(a)

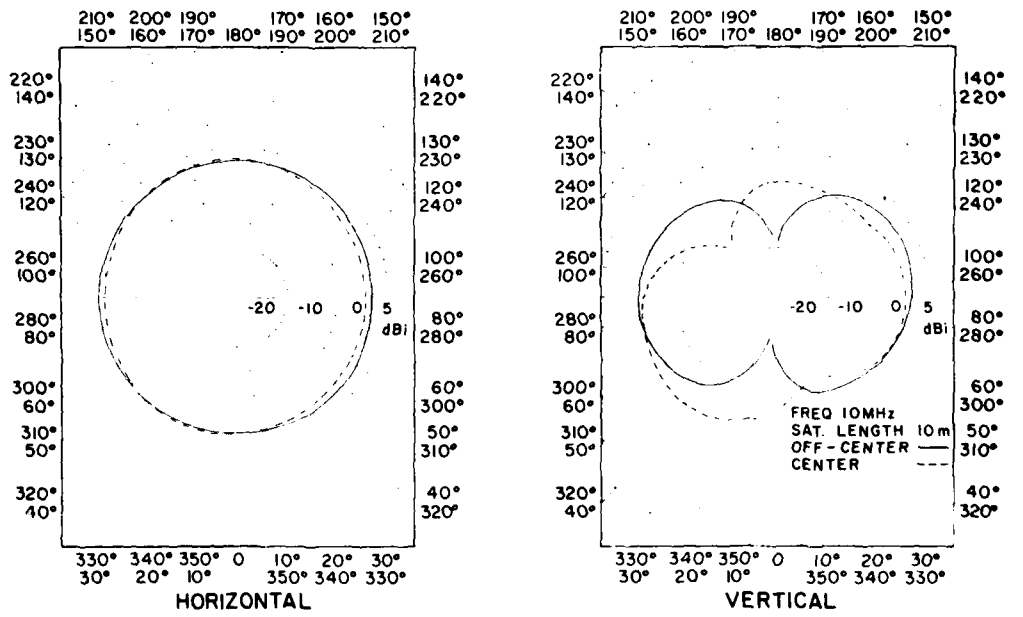

Figure 11(b)

Figure 11. Antenna Gain Patterns-Configurations a (Off-center) and b (center)

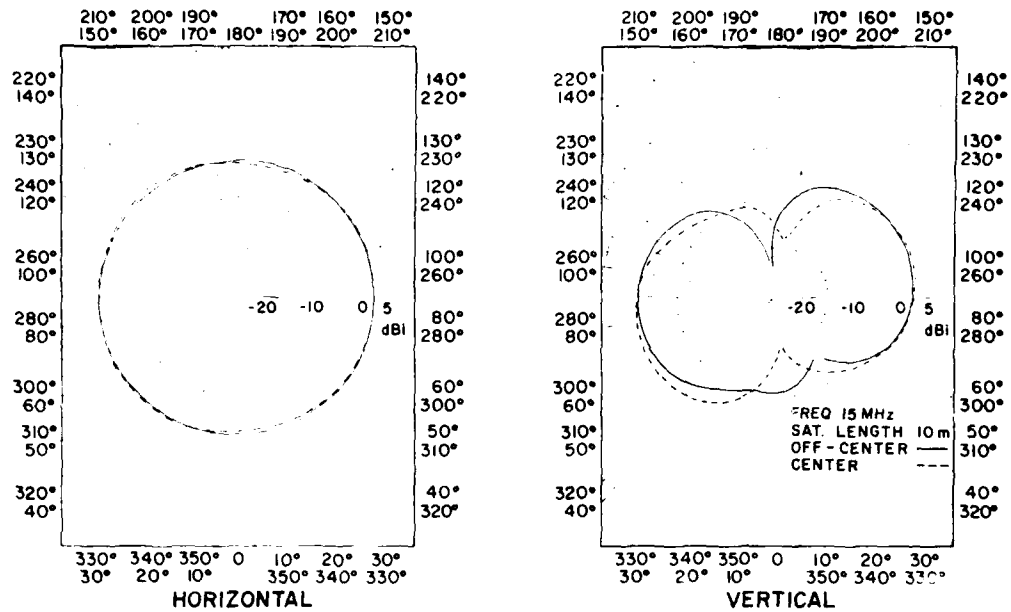

Figure 11(c)

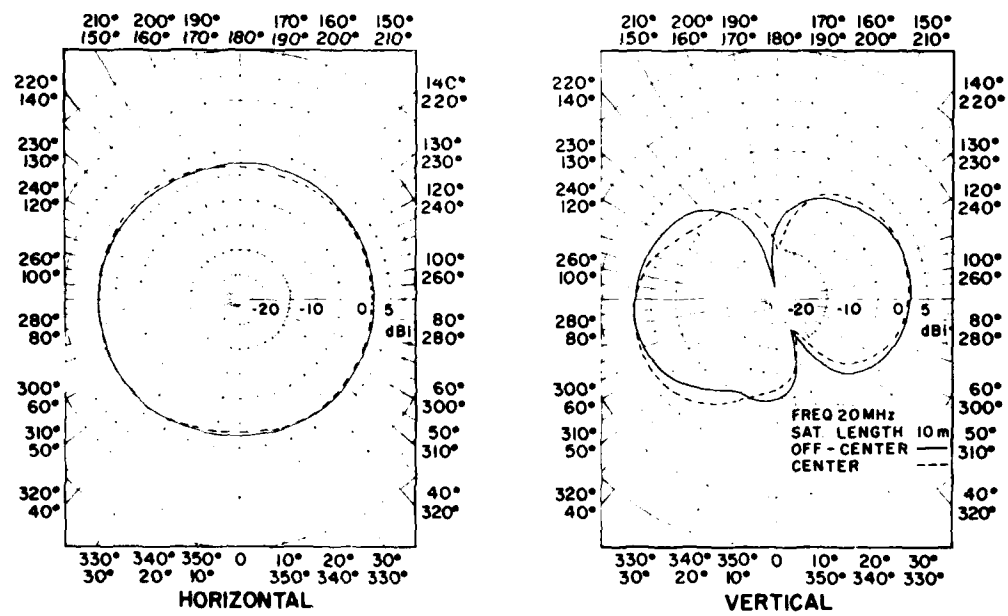

Figure 11(d)

Figure 11. Antenna Gain Patterns-Configurations a (Off-center) and b (center) (Contd)

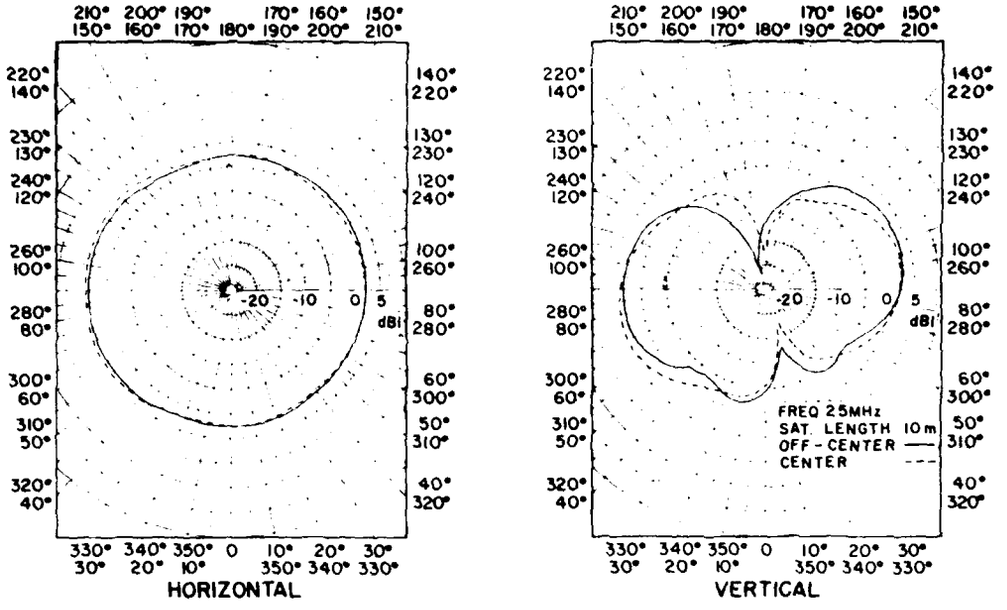

Figure 11(e)

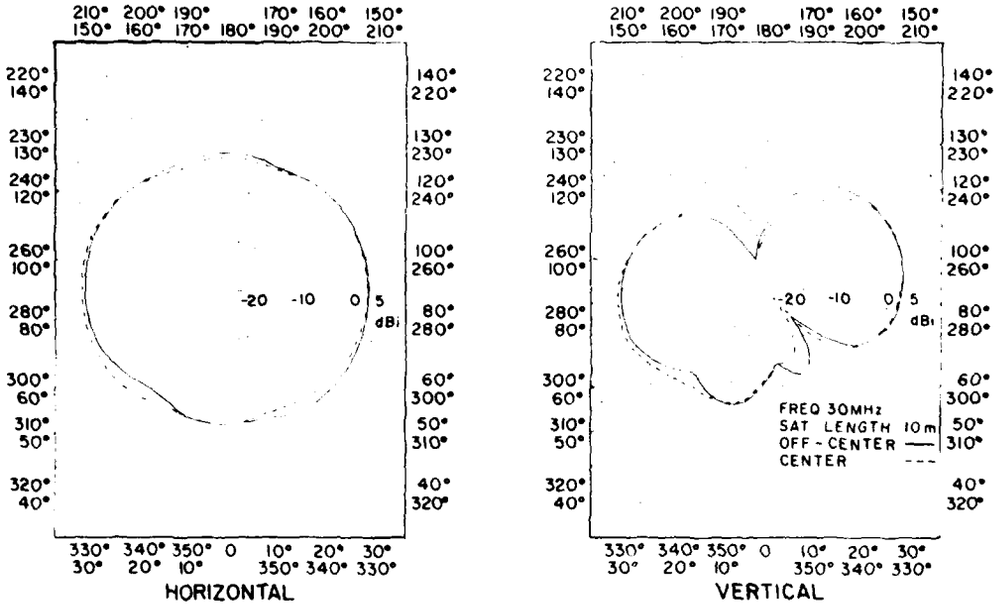

Figure 11(f)

Figure 11. Antenna Gain Patterns-Configurations a (Off-center) and b (center) (Contd)

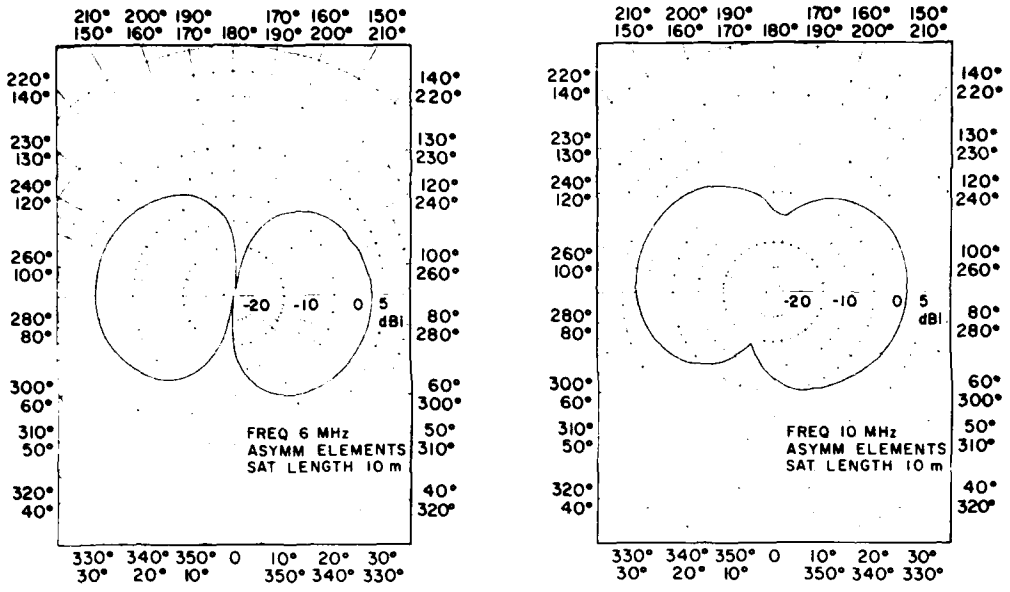

Figure 12(a)

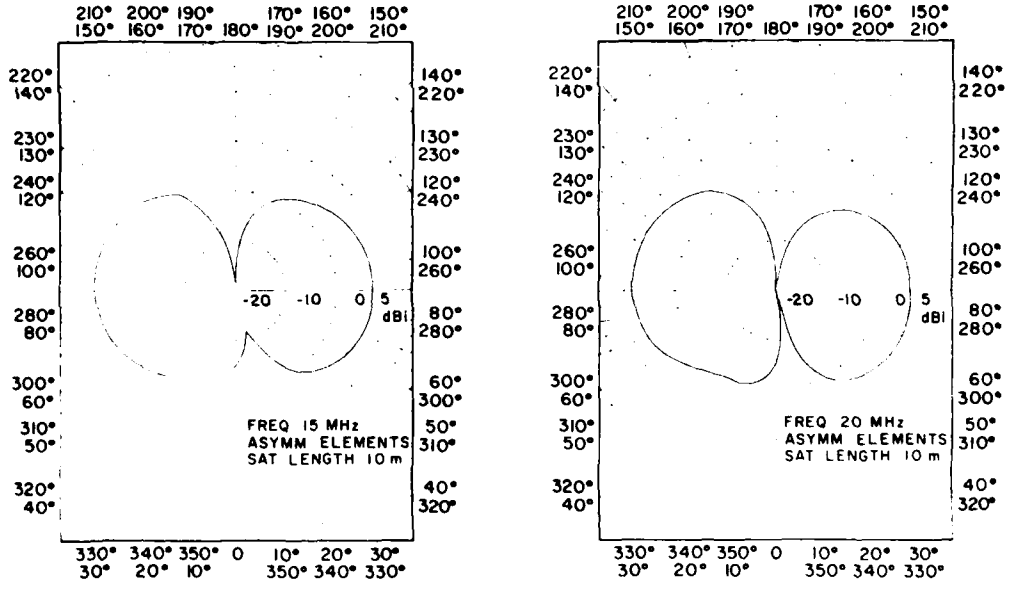

Figure 12(b)

Figure 12. Antenna Gain Patterns-Configuration c

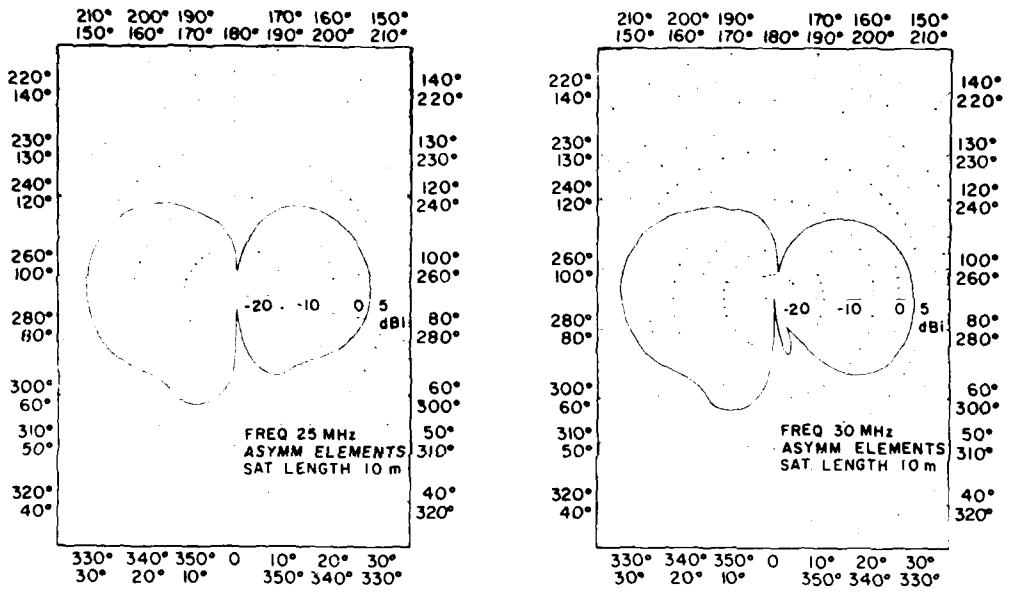

Figure 12(c)

Figure 12. Antenna Gain Patterns-Configuration c (Contd)

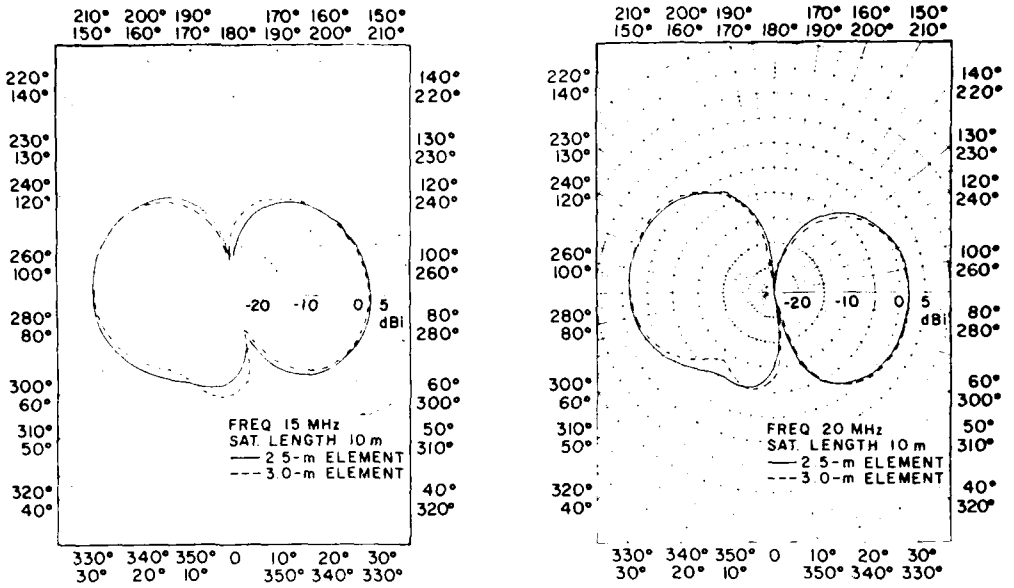

Figure 13(a)

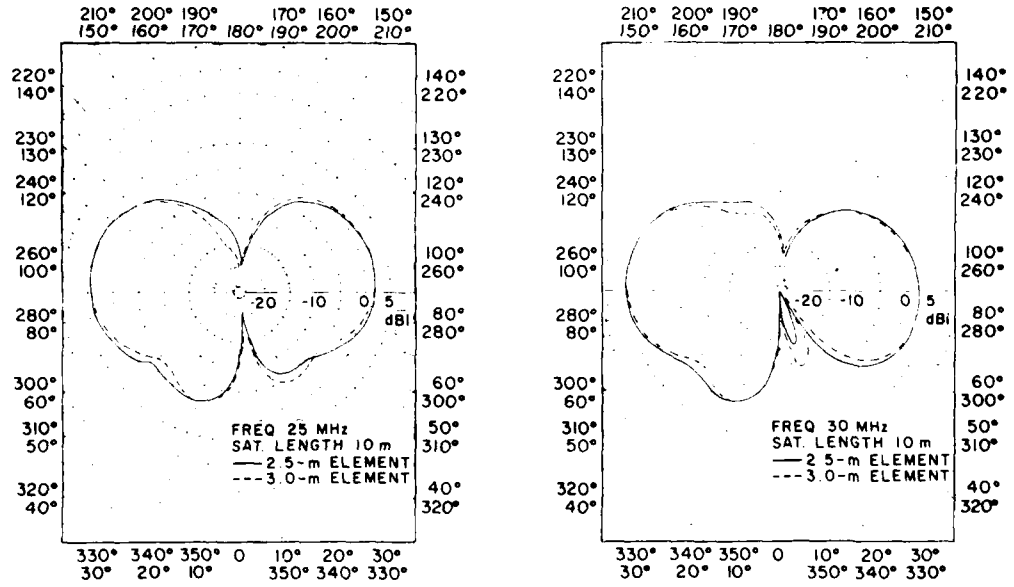

Figure 13(b)

Figure 13. Antenna Gain Patterns-Configurations d (2.5 m elements) and e (3.0 m elements)

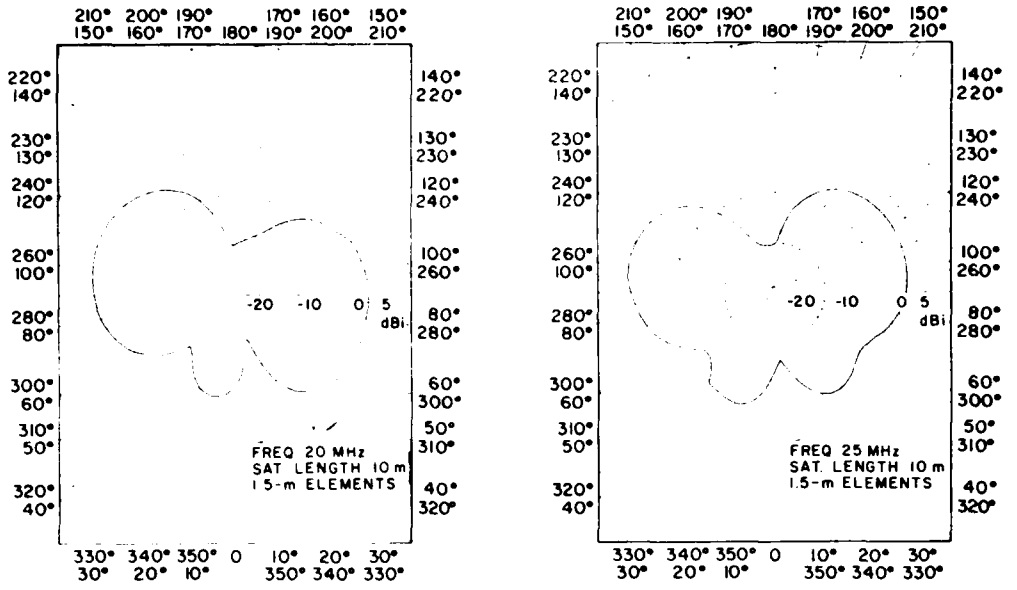

Figure 14(a)

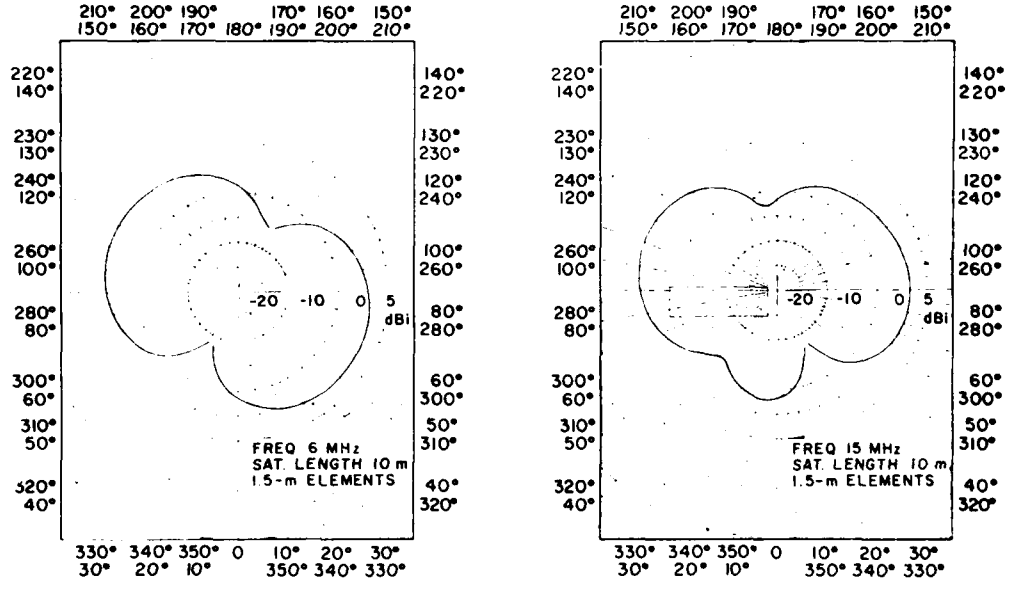

Figure 14(b)

Figure 14. Antenna Gain Patterns-Configuration f

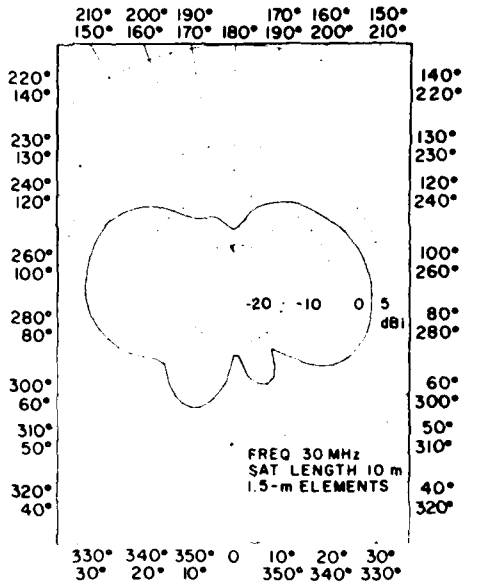

Figure 14(c)

Figure 14. Antenna Gain Patterns-Configuration f (Contd)

6. SIGNAL-TO-NOISE RATIO ANALYSIS

An antenna will deliver the maximum signal power to a receiver when the load presented by the receiver is matched to the antenna impedance. This matching is important to maintain the signal-to-noise ratio (SNR) present at the antenna. The available signal power at the input of a receiver is proportional to the local field strength and the effective area of the antenna

$$P_A = \frac{A_e E^2}{120\pi} ,$$

where

P_A = available power

A_e = effective area (m^2)

E = electric field intensity (volts/m) ,

Under matched conditions

$$A_e = \frac{\lambda^2 G}{4\pi} \quad .$$

where

G = antenna gain .

If the antenna is not matched the available power[2] will be

$$P_A = \frac{A_e E^2 4R_A R_L}{120\pi |R_A + jX_a + R_L|^2} \quad .$$

where

R_A = resistance (antenna)

X_A = reactance (antenna)

R_L = resistance (load) .

The antenna is assumed to be connected to a transmission line terminated in a pure resistance. The fraction of power available from an unmatched receiving antenna is

$$\mu = \frac{4R_L R_A}{((R_L + R_A)^2 + X_A^2)} \quad .$$

External noise such as atmospheric or galactic is the background against which the desired signal must be detected. In this analysis man-made noise was not included, although this may be a factor considering satellite generated noise. At frequencies below 10 MHz atmospheric noise is clearly the dominant factor. HF noise levels have been reported in CCIR Report No. 322 (ITU)[3] and are given in terms of "f_a" defined as follows:

$$f_a = \frac{P_{av\ noise}}{KT_oB} = \frac{T_a}{T_o}$$

or Fa when stated in decibels.

---

2. Collin, R., et. al. (1969) Antenna Theory, Vol. 1, McGraw-Hill Book Company, N.Y.

3. (1964) CCIR Report No. 322 ITU, Geneva, Switzerland.

$$F_a = 10 \log_{10} \frac{P_{av\ noise}}{KT_oB} \quad ,$$

where

K = Boltzman's Constant = 1.38×10^{-23} Joules/^oK

P_{av} = noise power from perfect, short vertical monopole

T_o = reference temperature, 290 K

B = effective receiver noise bandwidth (Hz)

T_a = effective antenna temperature in the presence of external noise (degrees Kelvin) .

The minimum detectable signal is degraded when the gain of an antenna is not adequate to insure that the external noise delivered to the input is greater than the internal noise of the receiver. As the antenna gain is increased the external noise will increase until it reaches a level where the external noise is greater than the internal noise, and any further increase in gain no longer has any significant influence on the SNR ratio. The noise performance of a receiver is described by a noise figure F, defined as the ratio of the SNR ratio at the input to that at the output.

$$F = \frac{(S/N)_{in}}{(S/N)_{out}} = \frac{N_{out}}{GKT_oB} \quad ,$$

where

G = gain of system .

The effective temperature T_e of a network is defined as the input temperature that would account for the noise generated internally by the receiver[4]

$$T_e = T_o(F-1) \quad ,$$

where

T_o = 290 K .

4. Weekes, K. (1968) Antenna Engineering, McGraw-Hill Book Company, N.Y.

In terms of the effective temperature of the network (T_e) the noise output is

$$N_{out} = GKB(T_a + T_e) \quad ,$$

which is the sum of the input noise and the noise generated by the receiver.

If the antenna and receiver had conjugate matched loads, then

$$S/N = \frac{S_i}{KB(T_a + T_e)} \quad ,$$

where

S_i = power input signal .

Due to mismatch factor μ the S/N is changed to

$$S/N = \frac{\mu S_i}{KB(\mu T_a + T_e)} \quad .$$

This expression indicates that it is only necessary to ensure that the noise power (μT_a) reaching the first amplifier is high enough to override the receiver noise.

For the satellite antenna the desired condition is

$$\mu T_a >> T_e \quad .$$

This condition will ensure no degradation of the SNR by receiver noise. The noise figure F for the satellite receiver is estimated to be 12 dB. Then

$$T_e(dBK) = 10 \log [\, 290^{O}(15.85 - 1)] = 36.3 \text{ dBK} \quad .$$

Figure 15 shows the antenna temperature T_a as a function of frequency. These values were determined from CCIR Report 322[3] using only summer maxima, since the experiment is scheduled to start in March and end in September. Also on this plot is the equivalent noise temperature of the receiver. This shows the loss of received power due to a mismatch that can be tolerated before internal receiver noise seriously starts to effect the SNR, in terms of effective noise temperature T_e and antenna noise temperature T_a. The mismatch attenuation resulting from the various configurations were analyzed as a function frequency (Figure 16). These curves can be used to verify the condition

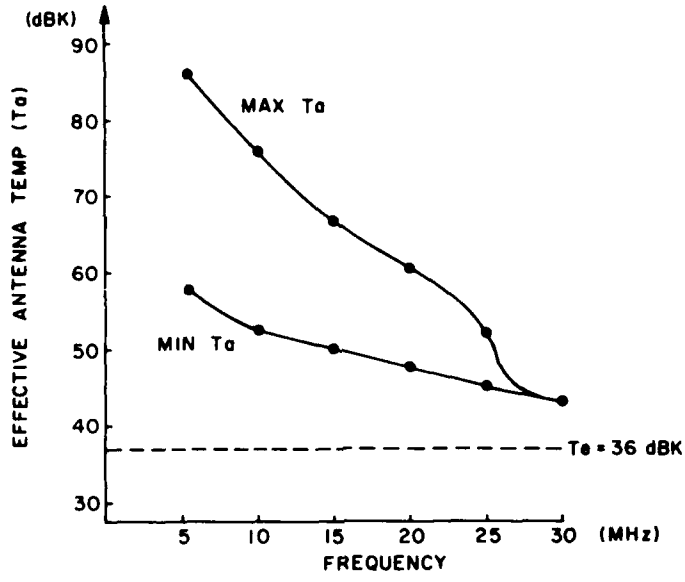

Figure 15. Effective Antenna Temperature vs. Frequency

$$\mu T_a >> T_e$$

for the antenna configurations analyzed when terminated in a load resistance of 50, 100, or 400 Ω, respectively. The least attenuation occurs over the frequency range of most interest, 15 to 30 MHz, for the antennas with elements of at least 3-m length using the load resistances shown.

7. ACTUAL ANTENNA STRUCTURE

The proposed actual satellite antenna will be constructed using two Storable Tubular Extendable Member (STEM) devices. The STEM is a tape of thin metallic material (beryllium copper), which takes on a cylindrical shape of high strength when allowed to extend. It can be stored in a minimum of space when coiled in flattened condition on a spool. The type used on the satellite is the Jack in the Box model (JBM).

Each element is in a canister, which is opened using a pyrotechnic device. When the canister opens, the strain energy will extend the coiled elements. The elements will then eject rapidly in the form of a spiral resulting in the extension of the overlapped STEM configuration.

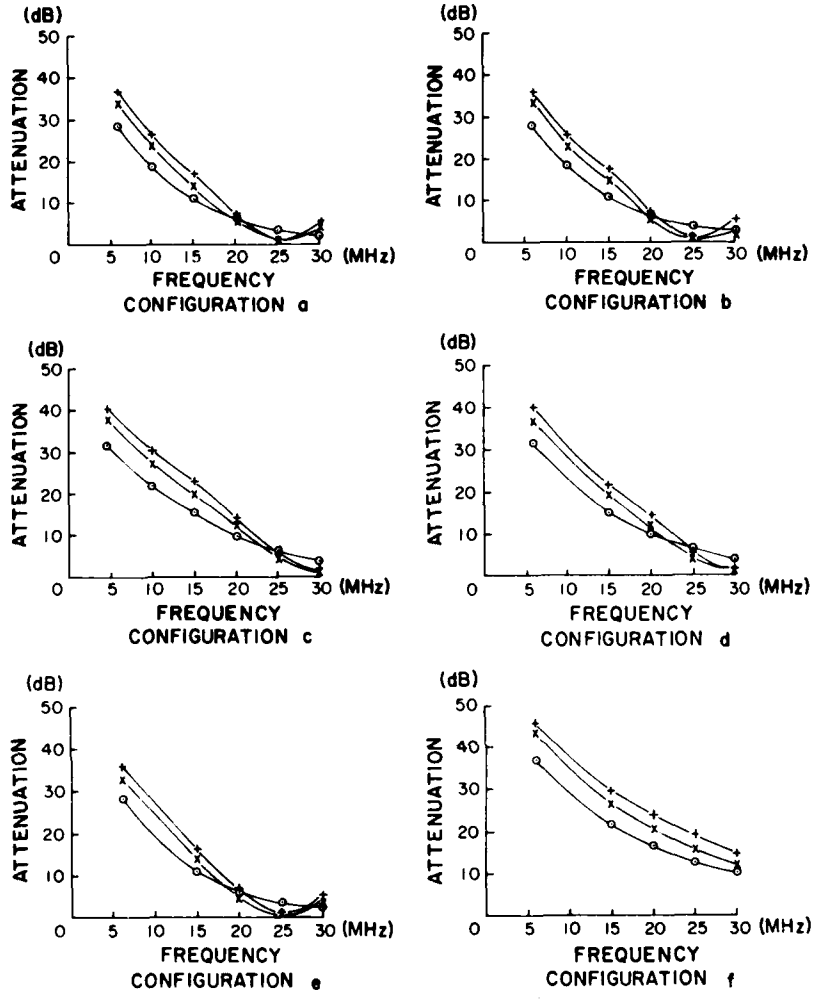

Figure 16. Mismatch Attenuation of the Various Antenna Configurations When Terminated in a Resistive Load. Load impedance: + = 50Ω, x = 100Ω, and ⊙ = 400Ω

8. IONOSPHERIC PLASMA

The satellite will be placed in a circular polar orbit, at an altitude of approximately 150 miles, where ducting is likely to occur. At this altitude the local ionospheric plasma will cause the antenna impedance to vary from its free-space value. This change may be quite significant at the lower end of the chosen frequency ranges, where the operating frequencies approach the plasma frequency.

AMP does not have the capability of calculating the impedance of an antenna immersed in a plasma, but it is important to get some estimate for the expected range of the changes in the impedance.

The impedance of a center driven dipole, short with respect to wavelength, can be expressed[5] as

$$R_A = 20\,\beta_o{}^2 h^2 \qquad (1)$$

$$X_A = \frac{-60\left(2\ln\left(\frac{2h}{a}\right)-3.39\right)}{\beta_o h} \quad \text{when} \quad \beta_o h \leq 0.5 \ ,$$

where

h = length dipole element
a = radius dipole element
$\beta_o h = \omega\sqrt{\mu_o \varepsilon_o}$
μ_o = permeability of free-space = 400πnH
ε_o = permittivity of free-space = 8.85 pF
ω = operating freq (rads/sec) .

When the value of $\beta_o h > 0.5$, the graphical representation of the King-Middleton expansion can be used to find the impedance of a dipole with a constant value for h/a, and $\beta_o h$ changing with frequency. The results from the King-Middleton theory are quite accurate for dipole antennas. The impedance of a dipole in free space[6] can be written as

$$Z_A = Z_o f(\beta_o h) \text{ (dipole free space)} \ , \qquad (2)$$

where

$Z_o = 120\pi$ (impedance of free space) .

This result does not include the effect of the refractive index of the ionospheric plasma

5. King, R. (1956) Linear Antennas, Harvard University Press, Cambridge, Mass.

6. King, R., et. al. (1961) The electrically short antenna as a probe for measuring free electron densities and collision frequencies in an ionized region, J. of Res. Natl. Bur. of Std 65(4):372.

$$\varepsilon_r = 1 - \left(\frac{\omega_p^2}{\omega^2}\right) , \tag{3}$$

where

ω_p = plasma freq (rads/sec)
ω = operating freq (rads/sec) .

The electron collision frequency at the altitudes considered is low when compared to the operating frequency and can be ignored. In a plasma the antenna impedance

$$Z_A(\text{dipole, plasma}) = Zf(\beta h) , \tag{4}$$

where

$$Z = Z_o \Big/ \sqrt{1 - \left(\frac{\omega_p^2}{\omega^2}\right)}$$

is the intrinsic impedance of the plasma. Since $f(\beta h)$ is a function of the electrical length of the antenna and

$$\beta h = \beta_o h \sqrt{1 - \left(\frac{\omega_p^2}{\omega^2}\right)} ,$$

the final expression for the antenna impedance in a plasma is

$$Z\ (\text{dipole, plasma}) = \frac{Z_o}{\sqrt{1 - \left(\frac{\omega_p^2}{\omega^2}\right)}}\ f\left(\beta_o h \sqrt{1 - \left(\frac{\omega_p^2}{\omega^2}\right)}\ \right) . \tag{5}$$

Allowing for the effect of the refractive index of a plasma when using the King-Middleton expansion, the obtained impedance corresponding to β_h is

$$Z' = Z_o f\, \beta_{oh} \sqrt{1 - \left(\frac{\omega_p^2}{\omega^2}\right)} . \tag{6}$$

The actual impedance of the antenna in the plasma is then

$$Z \text{ (dipole, plasma)} = \frac{Z'}{\sqrt{1 - \left(\frac{\omega_p^2}{\omega^2}\right)}} ,$$

which is the same expression as Eq. (5). In determining the impedance values, the region of the ionosphere, where the satellite will be operating, was assumed to have plasma frequencies of 4 to 12 MHz.

The impedance magnitudes calculated for a dipole antenna in a plasma, using the above described procedure are shown in Figure 17. For comparison, the impedance values for the free space antenna and the antenna configuration e are also shown in Figure 17.

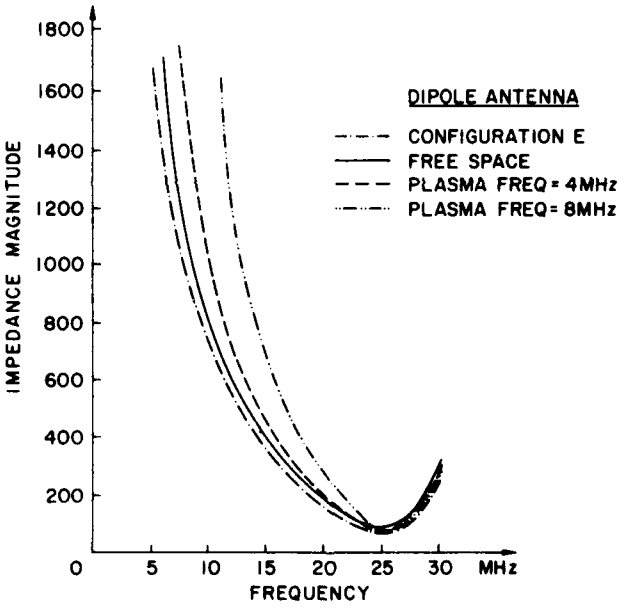

Figure 17. Impedance Magnitudes of a Dipole Antenna in an Ionospheric Plasma

The additional mismatch losses of a dipole in a plasma as compared to a similar antenna in free space are shown in Figure 18, for plasma frequencies of

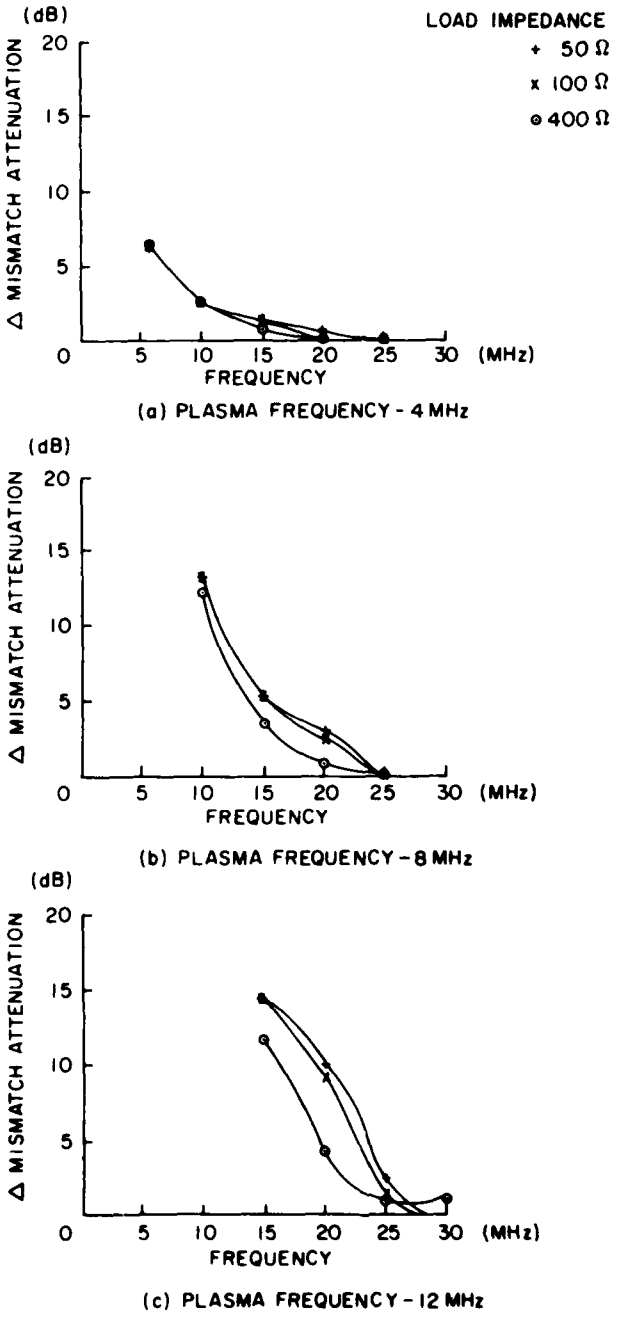

Figure 18. Additional Losses of a Dipole Antenna in a Plasma as Compared to a Similar Antenna in Free-space

4, 8, and 12 MHz. The mismatch losses increase with increasing plasma frequency, but the curves do indicate that 400 Ω is still a reasonable load value. The losses, calculated for the operating frequency range 15 to 30 MHz and a plasma frequency of 8 MHz, are less than 5 dB for the worst case (15 MHz). Plasma frequencies of the order of 12 MHz can be a problem in a 15 to 30 MHz operating frequency range (Figure 18c).

9. CONCLUSION

The calculations performed indicate that the satellite antenna with elements of at least 3 m long performed best overall. The dipole antenna configuration with an angled element has a good azimuthal pattern, but lacks the deep nulls in the downward direction on some frequencies. An asymmetrical configuration can have deep nulls in the downward direction. Specific location of the antenna on the satellite front bulkhead, does not have a major influence on the vertical positioning of the null axis. SNR ratio can present a problem if mismatch losses are too large to maintain the condition $\mu TA >> Te$. The mismatch losses for all configurations are the smallest when the antenna is terminated in a 400 Ω load. The influence of the plasma effect on the antenna impedance are small for frequencies of 8 MHz or less for the operating frequency band of most interest (15 to 30 MHz).

References

1. (1974) Antenna Modelling Program, Engineering Manual, MBA, San Roman, California.
2. Collin, R., et. al. (1969) Antenna Theory, Vol. 1, McGraw-Hill Book Company, N.Y.
3. (1964) CCIR Report No. 322 ITU, Geneva, Switzerland.
4. Weekes, K. (1968) Antenna Engineering, McGraw-Hill Book Company, N.Y.
5. King, R. (1956) Linear Antennas, Harvard University Press, Cambridge, Mass.
6. King, R., et. al. (1961) The electrically short antenna as a probe for measuring free electron densities and collision frequencies in an ionized region, J. of Res. Natl. Bur. of Std 65(4):372.

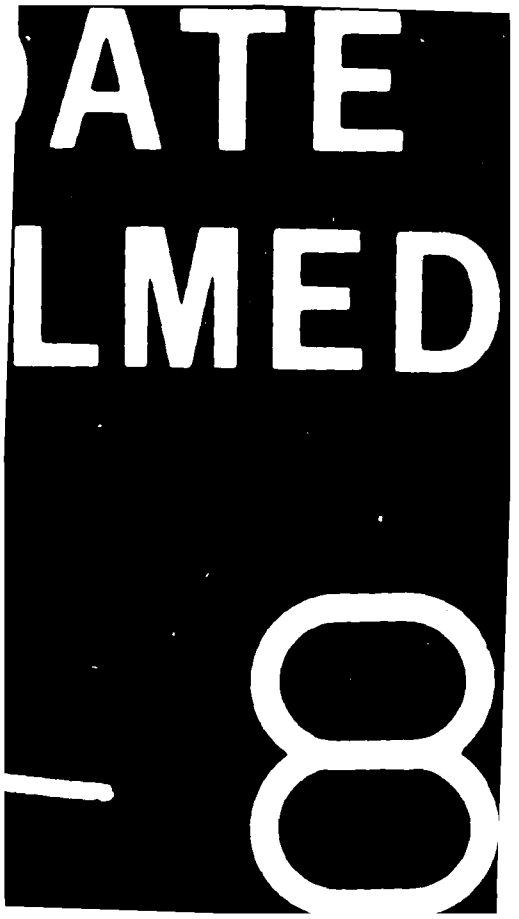
ATE
LMED
8